Ocean Engineering 283 (2023) 115122

Contents lists available at ScienceDirect

Ocean Engineering

journal homepage: www.elsevier.com/locate/oceaneng

Knowledge transfer strategy for enhancement of ship maneuvering model

Tongtong Wang *, Robert Skulstad, Motoyasu Kanazawa, Guoyuan Li, Houxiang Zhang

Department of Ocean Operations and Civil Engineering, Norwegian University of Science and Technology (NTNU), 6009 Aalesund, Norway

ARTICLE INFO

Keywords:
Knowledge transfer
Domain adaptation
Hybrid modeling
Trajectory prediction
Autonomous vessels

ABSTRACT

The advancement of autonomous vehicles and concerns about ship navigation safety have resulted in a greater need for ship model quality. However, in situations where there is limited prior information or data available about the system, the development of accurate models can be challenging. To address this issue, we propose a knowledge transfer strategy that can migrate and adapt domain knowledge from a well-modeled benchmark ship to a target ship. The benchmark, or source ship, should resemble the target ship in the feature space and reveal similar trends in the prediction horizon. By incorporating informative trends into the data-driven transfer function, the representative model of the target ship can be considerably enhanced. In this study, the experiments are conducted on two full-scale vessels that characterize different dimensions and dynamic properties. A feature vector is introduced to evaluate the configuration similarity between vessels, and ship maneuverability is compared to authorize the security of predictive tendency. The derived target ship model is verified to accurately predict maneuvering trajectories in various scenarios, demonstrating that knowledge transfer from a source ship facilitates the target ship modeling process. This approach provide new insights into the development of models for systems with confined information.

1. Introduction

With the better access to and sharing of digital data in marine traffic and vehicles, as well as the increasingly advanced technologies in data science, an intelligent era is dawning in the maritime industries. Digital twins are emerging as the next wave in modeling, simulation, and optimization technology (Zhang et al., 2022). They were introduced as a means of achieving efficient visualization and exchange of all digital content generated for an asset, and they vitally support ship life cycle service and operational decision-making.

Today's marine systems are operating in highly dynamic environments, and the twinship model has made it possible to estimate the current status of a vessel and its behaviors in interaction with such environments (Rasheed et al., 2020). Traditional physics-based models define how a vessel performs over time by means of complex ordinary differential equations derived theoretically, which are rational but do not account for noise and disturbances. Additionally, the fluid dynamic effects and the complicated geometry of the hull surface cause an asymmetrical behavior, increasing the difficulties in developing a ship dynamic model that perfectly reflects the complex system. Missing of details always happens when using equations to describe the marine system. Moreover, when estimating the key parameters in marine dynamics, it is challenging to get accurate representations from the noisy and disturbed experimental data (Sutulo and Soares, 2014; Wang et al., 2021b). A mismatch between parameters and the truth values will lead to the degradation of model quality.

For those vessels whose representations are not entirely known, there are probably different possibilities, each of which results in different models. For instance, if data-driven techniques such as neural networks are applied to approximate the ship dynamics (Li et al., 2017; Dai et al., 2012), a black-box model is much more likely to be derived. Such a model can deliver excellent solutions to represent the nonlinear complex system as long as sufficient high-quality data is available. However, these kinds of models have stringent requirement on the training data, and are always criticized for their limited interpretability and blank inspection of the underlying process (Solomatine and Ostfeld, 2008; Gunning et al., 2019). Thereby, if both the domain knowledge and data could contribute to the ultimate output, the performance of the hybrid model appears promising in terms of learning efficiency and explainability (Wang et al., 2021a, 2022). Because from the functionality point of view, the hybrid model integrates the advantages of both disciplines and turns to provide an inspiring solution to the challenging ship dynamics modeling task.

Driven by the desire to model the vessel with confined information, we proposed a hybrid approach with both domain knowledge and data incorporated. Specifically, for a surface vessel, the main principles and

* Corresponding author.
E-mail addresses: tongtong.wang@ntnu.no (T. Wang), robert.skulstad@ntnu.no (R. Skulstad), motoyasu.kanazawa@ntnu.no (M. Kanazawa), guoyuan.li@ntnu.no (G. Li), hozh@ntnu.no (H. Zhang).

https://doi.org/10.1016/j.oceaneng.2023.115122
Received 27 March 2023; Received in revised form 9 June 2023; Accepted 13 June 2023
Available online 25 June 2023

mass distributions are much easier to get than the nonlinear damping terms related to the water viscosity, ship hull shape, ship movement relative to the water, etc. But the damping influence is not ignorable in deriving position projections into the future. Instead of spending lots of effort to estimate the specific hydrodynamic parameters of the target ship, we propose an approach to transfer and adapt domain knowledge leveraged by an existing benchmark ship. The benchmark ship, which preserves and reveals prior knowledge on maneuverability, is called the source ship. To enable the knowledge transfer process, the source ship S is required to resemble the target ship T in both the geometry and dynamic domains, i.e.,

$$S \cap T \neq \varnothing \tag{1}$$

The source and target ships both follow the kinematics and rigid-body kinetics policies when maneuvering. As they both move in six degrees of freedom (DOFs), their motions are governed by the same Newton-Euler formulation (2), where different matrices and vectors and their properties will be defined accordingly. The control force τ due to a propeller, a rudder, or a fin is expressed in a general form, $\tau = ku$, where k is the force coefficient and u is the control input depending on the actuator considered. The environmental forces are also approximated in a general form parameterized to the ship considered.

$$\boldsymbol{M}\dot{\boldsymbol{\nu}} + \boldsymbol{C}(\boldsymbol{\nu})\boldsymbol{\nu} + \boldsymbol{D}(\boldsymbol{\nu})\boldsymbol{\nu} + \boldsymbol{g}(\boldsymbol{\eta}) + \boldsymbol{g}_0 = \boldsymbol{\tau} + \boldsymbol{\tau}_{\text{wind}} + \boldsymbol{\tau}_{\text{wave}} \tag{2}$$

Based on our physical insights into the surface vessel systems, it is reasonable to infer that joint domain knowledge enables the source ship to reveal future evolution for the target ship. Yet the mismatch between the approximations by the source model and the ground truth must exist because of the distinctions between the two agents. It is known that slight changes in ship geometry will lead to different hydrodynamic properties. Thus, it is pretty likely that the state variables $\mathbf{x}$ of two systems will not be identically distributed.

Based on the informative domain knowledge leveraged by the source ship, a data-driven transfer function is introduced for domain adaptation. Benefiting from the domain knowledge, the training process can be achieved with only limited data. From the modeling perspective, the proposed knowledge transfer methodology provides new insights for those ships whose either accurate dynamic models or large quantities of operational data are available to construct purely physics-based or data-driven models. It reuses the knowledge acquired from other well-established models and requires only limited data inputs to achieve good enough models easily. Meanwhile, the incorporation of prior knowledge brings a better understanding of the causal relationships of the system and offers possibilities for inspection.

In this study, the offshore supply vessel, Olympic Zeus, serves as the test bed. It was built by Ulstein Verft AS and launched in 2009. The vessel is equipped with two main propellers, one retractable thruster forward, four side tunnel thrusters—two forward and two aft (Ulstein, 2022). The source ship adopted in this study is the research vessel (R/V) Gunnerus, which is owned and operated by the Norwegian University of Science and Technology (NTNU). Launched in 2006, the ship operates as an experimental platform for a variety of activities within the marine domain (NTNU, 2022). The R/V Gunnerus was originally equipped with twin fixed-pitch ducted propellers and rudders and one tunnel thruster from Brunvoll. It went through a thruster refit in 2015, and the original propellers were replaced with azimuthing thrusters. However, to increase the configuration similarity between target and source ships, we would use the ship model before conversion as the source.

Though the target and source vessels are designed with different principal dimensions, propulsion plant, and mission requirements, they are believed to have comparable feature space. The knowledge transfer across ships and its effect on enhancing hybrid modeling will be investigated in this study. The major contributions are as follows:

- The knowledge transfer framework across ships is proposed based on both model-based and data-driven disciplines. A benchmark ship is occupied with providing instructive prior knowledge for the target ship. The characteristics vector is introduced to evaluate the geometry and dynamic properties similarity among ships.
- The physics-data hybrid modeling approach is proposed to increase model quality for vessels with incomplete information. A comparison experiment between the proposed model and traditional neural network model is conducted.
- Experiments are conducted on two real ships to validate the modeling framework.

The overall organization of the paper is as follows. Recent and related work of machine learning and transfer learning in the maritime domain is introduced in Section 2. Section 3 introduces the proposed modeling framework and the criteria for evaluating the ship characteristic consistency. Section 4 presents firstly the maneuverability properties of the two vessels. The predictive performance of the transfer learning approach and traditional recurrent neural network model are compared in this section. The experimental results are discussed in Section 5. Section 6 concludes the paper.

2. Related work

For most of the cases where the absolute vessel dynamic models are absent, the motion prediction task has to be fulfilled by the data-driven methods. The following introduces traditional machine learning and transfer learning methods applied in the maritime domain.

2.1. Traditional machine learning

Machine learning (ML) approaches have been prominent in the literature historically. Various algorithms are employed to develop ship models for control or prediction purposes. Owing to the excellent approximation capabilities of neural networks (NNs), they are widely used for scenarios subject to unknown dynamics and environmental uncertainties, such as motion prediction (Yin et al., 2018), trajectory tracking (Dai et al., 2015), path following Shin et al. (2017) and Zheng and Sun (2016), docking (Qiang et al., 2019), and dynamic positioning (Skulstad et al., 2019). Besides, unsupervised ML algorithms are often applied to collision avoidance issues with the perception of encounter situations (Wang et al., 2020). In the system awareness space, ML also brings significant value. Numerous NN examples exist in the marine context beyond motion prediction, and they are highly prominent in the field. For example, a recurrent NN based on long–short-term memory (LSTM) was used to deal with the hidden latent state of the unmanned surface vehicles (Woo et al., 2018). Similarly a radial basis function (RBF) network was constructed with the aid of a sliding data window to predict ship roll dynamics (Yin et al., 2018). These examples are perceived as black boxes where the input and output dependencies are simulated implicitly. For those cases where the model structure is known beforehand, the ML is alternatively used to decide uncertain parameters. The support vector machine (SVM), as well as the Gaussian Process (GP), are gaining popularity for addressing system identification issues (Wang et al., 2021b; Ramirez et al., 2018).

In the maritime context, researchers are proposing abundant efficient learning algorithms, pre, and post-processing techniques to improve performance. For example, one can determine the learning features of NNs by sensitivity analysis or diminish the colinearity of hydrodynamic parameters by optimizing the training data. The uncertainties from model plants and environments have been well-stressed in these ML studies. The general procedure of traditional machine learning, either supervised or unsupervised, takes the form of labeling (or not), training, validating, and testing. The models are learning the experience included in the training dataset and are trained to manipulate a specific task. While if the dataset is less well-annotated or new scenarios are exposed, the conventional ML has to retrain the model. Failing this will make the model increasingly unfit to the learning task.

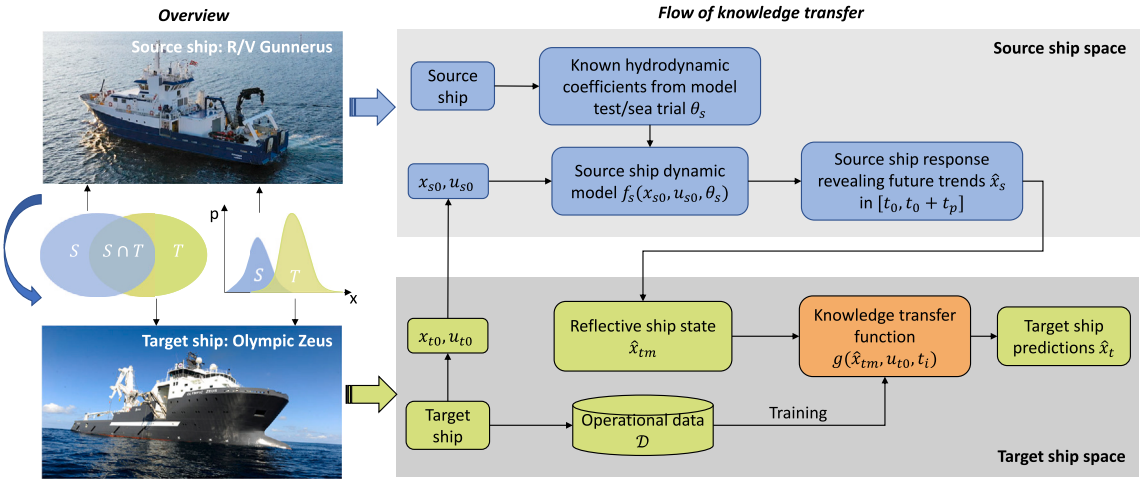

Fig. 1. The knowledge transfer flow across ships with different configurations. The source and target ships are assigned two real-world vessels—Research Vessel Gunnerus (NTNU, 2022) and Olympic Zeus (Ulstein, 2022), respectively. The target ship is 93.8 m long with four tunnel thrusters, and two main propellers installed, and the source ship is 31.25 m long and equipped with twin propellers and rudders.

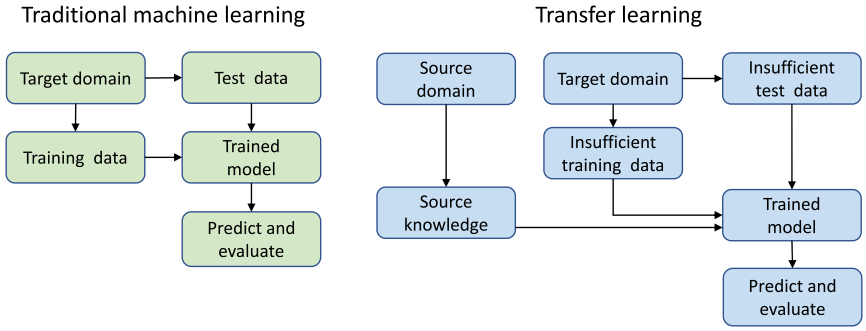

Fig. 2. The learning strategies of ML and TL.

2.2. Transfer learning

Transfer learning (TL) is inspired by the human ability to reuse knowledge from tasks they have completed before rather than learning all new tasks from scratch. ML algorithms require that training data be independent and identically distributed with the test data to deviate compromises the generalizability of the model. By contrast in TL, the restriction is relaxed. Thus it is widely used to solve data sparsity as well as domain adaption problems (Tan et al., 2018). For example, in fault diagnosis, labeled fault data acquisition is always an obstacle, and identical distributed features are rare in real-world applications. As a result, traditional ML typically will not serve our needs, and the cross-domain fault diagnosis using TL is becoming a popular choice (Yan et al., 2019). Zheng et al. (2019) summarized the existing works on diagnosing faults across domains and clarified the transferring strategies as well as the application objects.

Another field where TL is successfully applied is visual recognition. To ensure marine surveillance and navigation security, accurate ship detection in complex contexts has been an essential component. Deep learning (DL) methods, such as convolutional neural networks (CNNs), have been prominent for discriminating optical images. The applications of deep transfer learning in ship detection can be found in Li et al. (2019) and Wang et al. (2018). Moreover, it is widely used in water pollution (Panwar et al., 2020) and oil spill detection (Yekeen et al., 2020). As shown, most of the aforementioned applications stem from the desire to handle insufficient training data or the mismatch of task distribution regarding the ML or DL. Surveys (Tan et al., 2018; Pan and Yang, 2009) have divided the TL into different categories with the relationship between the source domain and target domain. The learning strategies of traditional ML and TL are distinguished in Fig. 2.

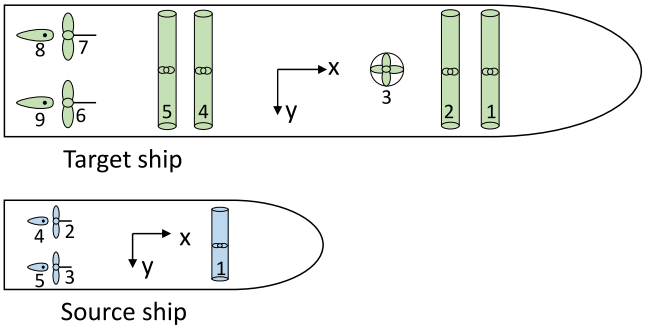

Fig. 3. The different dimensions and thruster layouts of the target and source ships.

3. Methodology

3.1. Overview

Consider a target ship whose nonlinear representation $\dot{\mathbf{x}}_t = f_t(\mathbf{x}_t, \mathbf{u}_t)$ is explicitly absent. $\mathbf{u}$ is the control input, which is assumed to be constant over the sampling interval, and $\mathbf{x}$ is the ship state vector containing position and velocity variables. There is also a source ship with a high-fidelity representative model $\dot{\mathbf{x}}_s = f_s(\mathbf{x}_s, \mathbf{u}_s)$. Given the discrepancies in geometry and propulsion configuration between ships, the ship state variables are distributed differently. By migrating and adapting the domain knowledge preserved by the source ship to the target ship with limited data, the target ship model is then constructed.

The knowledge transfer framework is proposed and presented in Fig. 1. As this figure shows, the upper layer is the source domain where the source ship dynamic is constructed and numerically solved, and the lower layer reflects the target space where the ship data is sampled and the nonlinear transfer functions. Assume that the target ship forecasting is triggered at time t_0, the ship status and control signals are recorded as $\mathbf{x}_{t0} = [x, y, \psi, u, v, r]$ and $\mathbf{u}_{t0} = [n_{pt}, \delta_{pt}, n_{st}, \delta_{st}]$, respectively. $[x, y, \psi]$ refers to the ship north and east positions and its heading angle. $[u, v, r]$ is the velocity vector, including the surge, sway, and yaw speed. n and δ are the propeller revolution and rudder position, pt and st indicate port side and starboard side, respectively. To ensure the initiation states and control signals are within the source ship physical range, linear transfer functions $l_x(\cdot)$ and $l_u(\cdot)$ are introduced as (3). It functions in a model-based way by non-dimensionalizing the states and commands in the target domain and dimensionalizing the non-dimensional variables back in the source domain.

$$\begin{aligned}\mathbf{x}_{s0} &= l_x(\mathbf{x}_{t0}) = \frac{\mathbf{x}_{t0}}{\Gamma_t}\Gamma_s \\ \mathbf{u}_{s0} &= l_u(\mathbf{u}_{t0}) = \frac{\mathbf{u}_{t0}}{\mathbf{u}_{t_{max}}}\mathbf{u}_{s_{max}}\end{aligned} \tag{3}$$

where $\Gamma_t = [L_t, L_t, 1, U_t, U_t, U_t/L_t]$, $\Gamma_s = [L_s, L_s, 1, U_s, U_s, U_s/L_s]$. U and L are the ship design speed and ship length. The subscripts s and t indicate source ship and target ship. To implement the linear transfer function, the control vector and state vector of the two systems should have the same dimension.

In order to ensure the domain knowledge is readily transferable, the source ship is required to meet the prerequisites such that it functions analogously to the target ship, and meanwhile, the model plant $f_s(\cdot)$ and hydrodynamic parameters θ_s are known beforehand. The source model is generally estimated and validated through model tests or sea trial experiments. Once the source model is properly prepared, the transmitted variables $\mathbf{x}_{s0}, \mathbf{u}_{s0}$ are fed into it. By numerically iterating the source model (4) forward, the ship response $\hat{\mathbf{x}}_s$ over the prediction horizon t_p is obtained. It is noted that the state $\hat{\mathbf{x}}_s$ is relative values with respect to the initiation state $\mathbf{x}_{s0}$.

$$\hat{\mathbf{x}}_s = f_s(\mathbf{x}_{s0}, \mathbf{u}_{s0}, \theta_s) \tag{4}$$

Then, the forecastings are transversed back to the target ship domain by:

$$\hat{\mathbf{x}}_{tm} = l_x^{-1}(\hat{\mathbf{x}}_s) \tag{5}$$

With the linear transformations across the source and target domain successfully performed, the instructive trends $\hat{\mathbf{x}}_{tm}$ are leveraged to the target ship. Nonetheless, considerable discrepancies between the trends and their true states still exist since the nonlinear hydrodynamic effects, which are not to be ignored in the ship maneuver model, have not been accounted for in this process. The nonlinear knowledge transfer function $g(\cdot)$ derived by the neural network acts to adapt the bias to the reflective ship states $\hat{\mathbf{x}}_{tm}$, as shown in (6), where t_i is the prediction time stamp, $t_i \in [0, t_p]$. In the end, the relative predictions $\hat{\mathbf{x}}_t$ are transmitted to the global outcomes. In this way, the knowledge leveraged by the source ship is aggregated and adapted to the target ship domain with the model-based linear transfer function and data-driven nonlinear calibration function. Consequently, the motion prediction of the target ship is enhanced with the addition of the referenced ship dynamics.

$$\begin{aligned}\hat{\mathbf{x}}_t &= g(\hat{\mathbf{x}}_{tm}, \mathbf{u}_{t0}, t_i) \\ &= g(l_x^{-1}(f_s(l_x(\mathbf{x}_{t0}), l_u(\mathbf{u}_{t0}), \theta_s)))\end{aligned} \tag{6}$$

3.2. Target and source ship feature resemblance

As introduced in Section 1, the target ship and the source ship are assigned by two actual vessels in practice. Table 1 lists the main geometric and propulsive characteristics of the two vessels. The maneuverability of a ship is usually impacted by several essential parameters, such as the length-beam ratio, beam-draft ratio, block coefficient, etc. (Taimuri et al., 2020). Therefore, in order to use the leveraged information with reasonable confidence, the source ship is required to, at a minimum, have similar characteristic vectors to those of the target ship. The characteristic vector is introduced as (7) to evaluate the similarity among ships. Δ in the vector is the ship's volume.

$$\ell = [C_b, L/B, B/T, L/\Delta^{1/3}, Ar/L_{pp}T, D_p/T]' \tag{7}$$

To measure the correlation between the two ships' characteristic vectors, the similarity coefficient κ is employed.

$$\kappa(P, Q) = \frac{N\sum p_i q_i - \sum p_i \sum q_i}{\sqrt{N\sum p_i^2 - (\sum p_i)^2}\sqrt{N\sum q_i^2 - (\sum q_i)^2}} \tag{8}$$

where $p_i \in P$ and $q_i \in Q$ are the elements in each vector, and N refers to the sample size. The κ value ranges between −1 and 1, and the larger κ is, the stronger the association of the two vectors will be. $\kappa(\ell_t, \ell_s)$ is calculated to be 0.95, indicating that the two vessels' characteristics are quite similar. ℓ_t and ℓ_s are the characteristic vectors of target and source ships, respectively.

Aside from the feature consistency, the control modes of the two vessels also must be as close as possible. The thruster configurations of the source ship and target ship are clarified in Fig. 3. When maneuvering in the horizontal plane, either the source ship or target ship is overactuated. The target ship is controlled by the propellers (6, 7) and rudders (8, 9) in parallel mode. The revolution speed and blade pitch angles of propellers are controllable. Two sets of individually operated tunnel thrusters at the bow and stern of the vessel (1, 2, 4, 5) are operated by RPM commands and produce the lateral force. On the source ship, the two main propellers and rudders controlled by RPM and turning angles serve the propulsion, and the single tunnel thruster works the same way as the target ship. The specifications of thruster constraints are compared in Table 2. If the tunnel thrusters and the forward thruster are excluded from the control inputs of the target ship, the two vessels are manipulated in an identical way. In the following experiments, they both are operated by the RPM and rudder

Table 1
Main dimensions of target ship and source ship.

Descriptions	Parameters	Target ship	Source ship
Hull			
Length overall	L_{oa} [m]	93.8	31.25
Length between perpendiculars	L_{pp} [m]	82.7	28.9
Breadth middle	B [m]	23.058	9.6
Draught	T [m]	7.5	2.6
Block coefficient	C_b	0.694	0.569
Speed	U [knot]	17.5	9.6
Rudder			
Rudder area	A_r [m^2]	12.15	2.42
Propeller			
Diameter	D_p [m]	4.5	2
Number of blades	–	4	5

Table 2
Thruster operational constraints of ships.

Target ship				
Thruster	Type	Max	Min	Rate change
1,2	Tunnel thruster	204 RPM	−204 RPM	20.4 RPM/s
4,5	Tunnel thruster	276 RPM	−276 RPM	27.6 RPM/s
6,7	Main propeller	132 RPM	−132 RPM	13.2 RPM/s
		28.7 deg	−21.5 deg	1.44 deg/s
8,9	Rudder	45 deg	−45 deg	3.7 deg/s
Source ship				
Thruster	Type	Max	Min	Rate change
1	Tunnel thruster	–	–	–
2,3	Main propeller	203 RPM	−203 RPM	20.3 RPM/s
4,5	Rudder	45 deg	−45 deg	5.7 deg/s

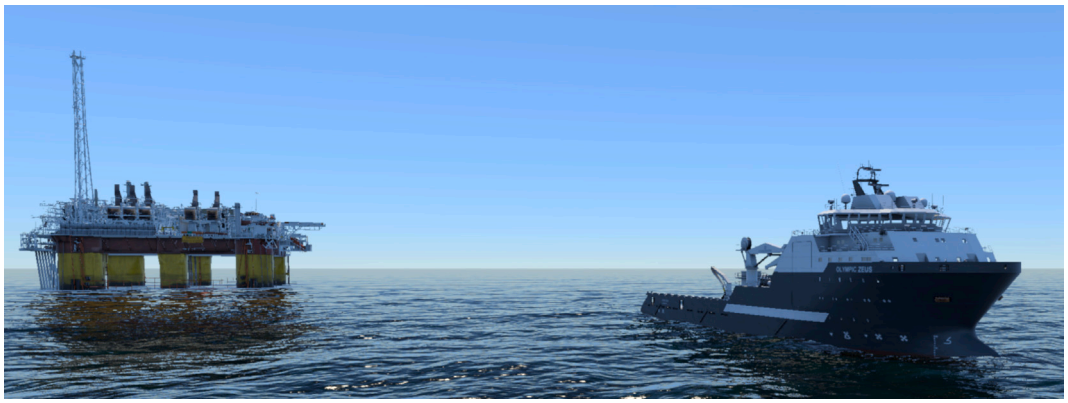

Fig. 4. A screenshot showing the simulated environment at offshore simulation centre.

angle commands, and the blade angle on the target ship is kept constant at the maximum value. From the analysis of the physical principles and control model, it is suggested that the source ship and target ship have common domain knowledge, and meanwhile, dissimilarities in features exist.

3.3. Dynamic model of source ship

The dynamic model of the source ship will be explained in the following context. The 3 degrees of freedom ship dynamic model, which considers the forces due to propellers, rudders, hull inertia, and friction, as well as the interaction effect between them, is constructed on the source ship file. The model is expressed as follows:

$$\begin{aligned} m(\dot{u} - vr - x_G r^2) &= X_H + X_R + X_P \\ m(\dot{v} + ur + x_G \dot{r}) &= Y_H + Y_R \\ I_z \dot{r} + m x_G (\dot{v} + ur) &= N_H + N_R \end{aligned} \tag{9}$$

where u, v, r represents the velocity in the surge, sway, and yaw direction. The subscripts H, R, and P on the right-hand side denote hydrodynamic, rudder, and propeller, respectively. m is the ship mass, x_G is the longitudinal position of gravity, and I_z refers to the inertial moment along vertical axis z which is measured positive down, and negative up.

The hydrodynamic force

$F_H = [X_H, Y_H, N_H]'$ is the hydrodynamic hull force due to the water inertia and friction, and it is approximated by the functions of u, v, r. In the total force model, these functions are described as the following polynomials using Taylor expansion.

$$\begin{aligned} X_H =& X(u) + X_{\dot{u}}\dot{u} + X_{vv}v^2 + X_{vr}vr + X_{rr}r^2 \\ Y_H =& Y_{\dot{v}}\dot{v} + Y_{\dot{r}}\dot{r} + Y_v v + Y_r r + Y_{r|r|} r|r| + Y_{v|v|} v|v| + Y_{r|v|} r|v| + Y_{v|r|} v|r| \\ &+ Y_{vrr} vr^2 + Y_{vvr} v^2 r \\ N_H =& N_{\dot{v}}\dot{v} + N_{\dot{r}}\dot{r} + N_v v + N_r r + N_{r|r|} r|r| + N_{v|v|} v|v| + N_{r|v|} r|v| \\ &+ N_{v|r|} v|r| + N_{vrr} vr^2 + N_{vvr} v^2 r \end{aligned} \tag{10}$$

where the hydrodynamic derivatives $X_{\{\cdot\}}, Y_{\{\cdot\}}, N_{\{\cdot\}}$, constituting the parameter vector θ_s, are estimated by model test. They have physical meanings corresponding to the zero frequency added mass effect, added mass Coriolis-centripetal forces, linear lift and drag, and cross-flow drag.

The propeller force

X_P is expressed as the generic formula (11) and parameterized to the R/V Gunnerus.

$$X_P = (1-t)\rho K_t D_P^4 n^2 \tag{11}$$

where ρ is the water density, K_t is the open water thrust coefficient of the propeller, and that coefficient relates to the advance coefficient J as (12).

$$\begin{aligned} K_t &= a_0 + a_1 J + a_2 J^2 \\ J &= u(1-w_p)/nD_p \end{aligned} \tag{12}$$

where D_P represents the propeller diameter and $(1-t)$ is the propeller deduction factor that is the interaction between hull and propeller. n is the propeller revolution, and w_p is the wake factor at the propeller position in maneuvering.

The rudder force

The forces induced by the rudder are calculated based on the lift force (F_L) and the drag force (F_D) as follows:

$$\begin{aligned} X_R &= F_L \sin\delta_i + F_D \cos\delta_i \\ Y_R &= F_L \cos\delta_i - F_D \sin\delta_i \end{aligned} \tag{13}$$

where δ_i is the hydrodynamic inflow angle of the rudder and is expressed as:

$$\delta_i = \arctan\left(\frac{v_R}{u_R}\right) \tag{14}$$

where u_R and v_R are longitudinal and lateral components of the rudder inflow speed as $V_R = \sqrt{u_R^2 + v_R^2}$. The lift and drag forces are written as:

$$\begin{aligned} F_L &= 0.5\rho A_R C_L V_R^2 \\ F_D &= 0.5\rho A_R C_D V_R^2 \end{aligned} \tag{15}$$

where A_R is the rudder area. C_L, C_D, as the lift and drag coefficient, are decided on the effective rudder angle $\alpha_R = \delta - \delta_i$, δ is the actual rudder angle. These coefficients are specified to the rudder profile, type, as well as geometry.

Numerical simulation

The source ship is numerically simulated by solving the dynamic model (9) with the Runge–Kutta fourth-order method. The iteration time step maintains consistency with the target ship data sampling frequency, and integration horizon is the same as prediction period t_p. In this case study, the target ship data is sampled at 10 Hz, and the prediction horizon is 30 s. The model trends $\hat{\mathbf{x}}_s$ over the prediction horizon t_p are reflected in the target space by (5). This way, the non-dimensional variables are successfully transferred back from the source domain to the target domain.

3.4. Neural network transfer function

Given the excellent approximate capability and simple architecture, the neural network appears to be a popular choice for estimating the nonlinear dependencies of input and output variables. In the knowledge transfer framework, a fully connected feed-forward NN structure is

Table 3
The target ship maneuver scenarios.

Datasets	Zigzag maneuver	Revolution percentage	Ship speed
Training datasets	10°/10° 20°/20°	53%	Slow
	10°/10° 20°/20°	91%	Fast
Test datasets	15°/15°	53%	Slow
	10°/10° 15°/15° 20°/20°	68%	Medium
	15°/15°	91%	Fast

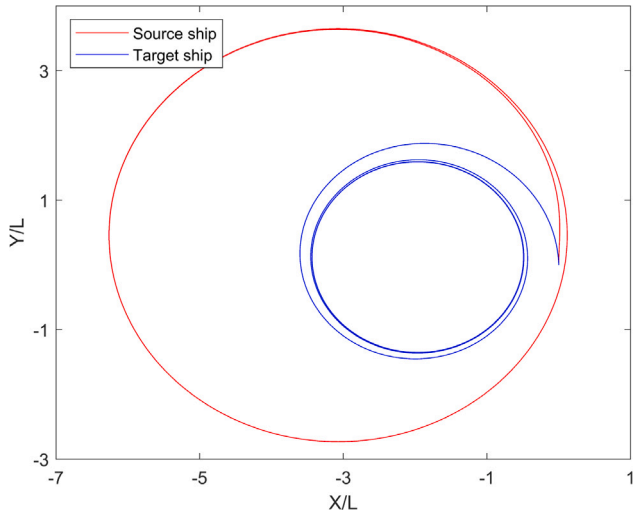

(a) The turning trajectories relative to its ship length.

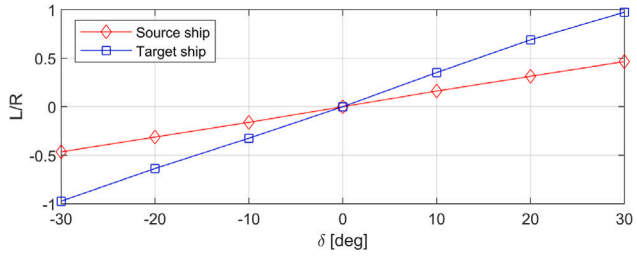

(b) The variation of steady turning radius against rudder angles.

Fig. 5. The turning capabilities of source and target ships.

adopted to transfer the instructive trends reflected by the source model to the target ship. The neural network is trained to minimize the error between the NN outputs and the labeled values by systematically adjusting the weights of each neuron.

The NN is structured with seven inputs, three outputs, and three hidden layers with 64, 64, and 32 neurons, respectively. The input space is constructed based on the source ship trends $[\hat{\psi}_{tm_i}, \hat{u}_{tm_i}, \hat{v}_{tm_i}, \hat{r}_{tm_i}]$, the prediction time stamp t_i, and the control signal RPM_0, δ_0 at initiation time. And the outputs are the target ship states sampled from maneuvering. The relative ship heading ψ_i, surge velocity u_i, and sway velocity v_i with respect to the initiation values are predicted. The training and test datasets for the NN are organized according to Table 3. In total, there are 170 trajectories included in the training datasets, and 129 trajectories distributed in five scenarios are applied to test the predictive performance. The data sampling frequency is 10 Hz.

The network is instantiated with the following settings. The activation function for the hidden layer is ReLu, and the weights are updated by Adam optimizer with the learning rate of 1×10^{-3}. The input values in the training set are normalized with a standard scalar, and the

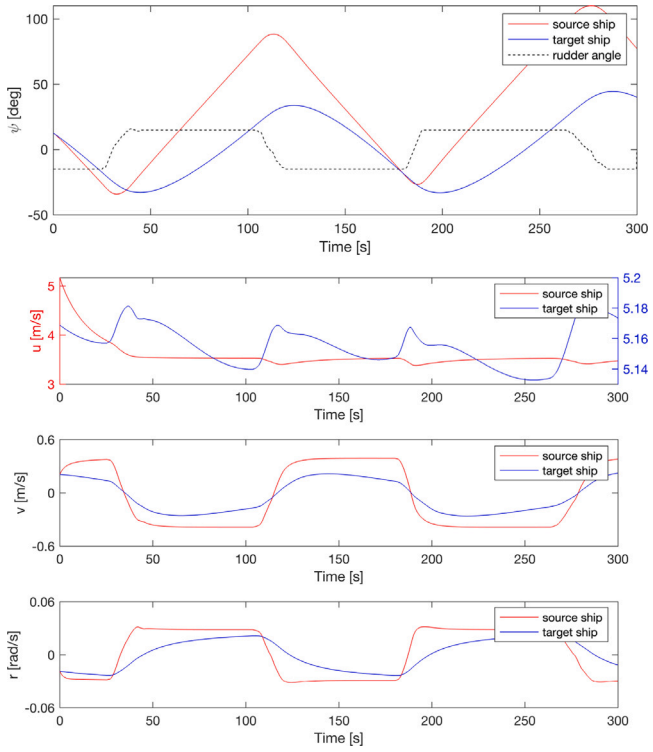

Fig. 6. Zigzag maneuverability comparison between source and target ships.

corresponding normalization is also applied to the test sets. The training performance is evaluated by minimizing the mean square error metric between labels and predictions. The network is implemented by using Scikit-learn (Pedregosa et al., 2011) in Python.

4. Experiments and results

4.1. Ship maneuverability

As discussed in Section 3.2, the target ship and source ship own similar characteristic vectors. Thereby, they are expected to behave analogously to identical commands. To deploy the maneuverability consistency between the source and target ship and verify the physics leveraged from the source ship are informative, turning circle and zigzag maneuvers are executed. The target ship maneuvers are carried out in a commercial marine vessel simulator developed by the Norwegian company Offshore Simulator Centre (OSC) AS.[1] Fig. 4 is a screenshot showing the simulated environment at OSC. The source ship maneuvers are simulated by the dynamic model developed in Section 3.3.

An illustration of turning characteristic diversity is presented in Fig. 5(a). The ship is operated at a 20° rudder angle to the starboard and 91% propeller revolution percentage. In this figure, the turning trajectories of the source and target ship are each scaled based on their own length. Specifically, the steady turning radius variations with respect to the rudder positions are shown in Fig. 5(b), where the x labels represent the rudder angle towards the starboard or port side, and the y labels refer to the ratio of ship length and steady turning radius. It is found that the course-changing capabilities of the target ship, as well as the source ship, are labeled with different values but similar trends. Both are characterized by linear relationships between the rudder angle and turning radius, but the slopes are found to be different values.

[1] https://osc.no/.

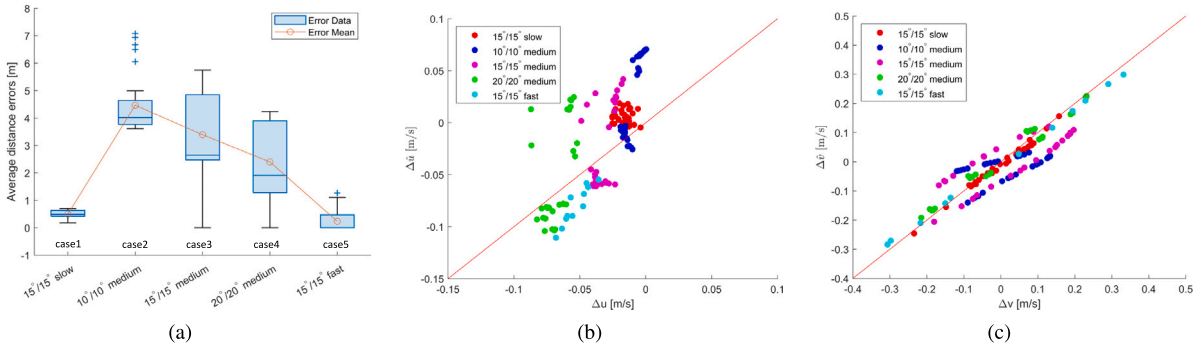

(a) (b) (c)

Fig. 7. Target ship predictions: (a) Average distance error, (b) Relative surge velocity, and (c) Relative sway velocity.

When the target ship executes zigzag, the source ship is simulated with identical commands. The ship headings, as well as the velocities of the surge, sway, and yaw, are shown in Fig. 6. It turns out that the source ship responds more quickly to the rudder change, but the velocities of both fluctuate in comparable patterns. In this case, the sampling frequency is 10 Hz, and the correlation coefficients of sway and yaw velocities are calculated to be $\kappa(v_s, v_t) = 0.97$, $\kappa(r_s, r_t) = 0.78$, indicating a strong correlation. Because of the physical constraints on the maximum approach speed, the divergence in the surge velocity is more obvious but still can be transferred as they are systematically biased.

4.2. Target ship motion prediction

To assess the predictive accuracy, the average distance error is introduced as (16).

$$e = 1/N \sum_{i=1}^{N} \sqrt{(x_i - \hat{x}_i)^2 + (y_i - \hat{y}_i)^2} \tag{16}$$

where x_i and y_i are the accurate target ship positions, and $\hat{x}_i$ and $\hat{y}_i$ are the hybrid predictions.

Five zigzag scenarios under different speeds and execution angles, as indicated in Table 3, verify the generalization capability of the hybrid model. The average distance errors are presented as Fig. 7(a), where slow, medium, and fast correspond to the three different revolution percentages. The predictive performance of the 15°/15° slow scenario is observed to be the best, and that of the 15°/15° fast is pretty close. In the medium speed group, the average errors become visibly more enormous, and the mean value decreases as the execution angle increases. Comparing the mean errors of case 1, 2, 4, and 5, although these four scenarios all have at least one control variable that is covered by the training data, the divergences of case 1 and 5 are much lower than that of case 2 and 4. These findings indicate that the ship approach speed contributes more when predicting.

Figs. 7(b) and 7(c) exhibit the predicted relative surge and sway velocities against the target actual states. The velocities shown in the figure are the relative values with respect to the initiation states, i.e., $\Delta u = u - u_0$, $\Delta\hat{u} = \hat{u} - u_0$. From the two figures, it is evident that the sway velocities are generally forecasted with higher accuracy. While in the surge velocity predictions, more outliers are spotted. In each scenario, two clusters could be roughly separated above and below the red line, which might be distinguished by the direction of the rudder position.

To present the strength of knowledge transfer framework in dealing with insufficient data, we constructed a traditional recurrent neural network (RNN) to predict future ship trajectories. The Long–Short Term Memory (LSTM) networks, as a special kind of RNN, are particularly good at learning long-term dependencies and processing time-series forecasting because they work to retain useful information about previous data in the sequence instead of treating each data point independently. Thus, we applied the LSTM for nonlinear ship motions multi-step prediction.

When constructing the predictive ship model, the input space contains the historical ship states, the output is the ship velocities sequence with length of prediction horizon t_p. The network is trained on the same data set as Table 3 shows. The network structure contains one input layer, one LSTM layer with 256 units, one fully connected layer, and one output layer. Standardization is performed before data are fed into the network. The model is compiled using the Adam optimizer with the mean squared error loss function. The network is trained 1000 epochs under the machine learning framework of TensorFlow.

Fig. 8 displays one prediction instance in test case 5 — 15/15 fast zigzag maneuver. It contains the predictions of surge velocity, sway velocity, and heading angle given by different approaches from left to right. The x-axis represents the prediction time horizon, which is 30 seconds in our experiment. It is seen that the results got from the proposed approach match better than the LSTM, and the LSTM predictions show more divergence, especially in surge directions. An illustration of the target ship trajectory predictions using different methods is presented in Fig. 9. Fig. 9(a) contains five figures, each showing the predicted trajectories when the rudder turns towards the starboard. The red dot indicates the initiation position where the prediction is triggered, and the blue lines refer to the LSTM predictions. The red line reflects the target ship's true states and the green line presents the predicted states of the proposed approach. The ultimate positions of each prediction are marked with star signs. In terms of target ship predictions using the transfer learning approach, the 15°/15° zigzag at slow speed has the most satisfying performance, and the predictions diverge most in the 10°/10° zigzag at the medium speed. The results when the ship rudder is reverted to the portside are presented in Fig. 9(b). From these test scenarios, it is seen that the transfer learning predictions show better accuracy than the traditional LSTM network. The statistical results, including velocity, heading angle, and distance errors during the forecast, are presented in Table 4. It is observed from the table that the LSTM model error at surge direction is more significant than that of the proposed model, but the errors at sway direction are smaller. Since the sample size is limited, the LSTM model is prone to be overfitting, and difficult to get good generalization capability on the test scenarios. We believe that there is space to improve the LSTM performance if more data is given. While sometimes it is difficult to provide enough representative data in reality. Thereby, the transfer learning approach benefiting from the prior knowledge is promising, and our proposed approach verified the effectiveness through the experiments. Moreover, the learning process of the knowledge transfer approach is less complicated than the LSTM model. In our experiment, the proposed model converged quickly (within 15 s) to small variations around the true values, but the LSTM model took 281.83 s to finish 1000 epoch training on the same computational device. Through the experiments, the effectiveness of the knowledge transfer framework and hybrid modeling approach is evidenced.

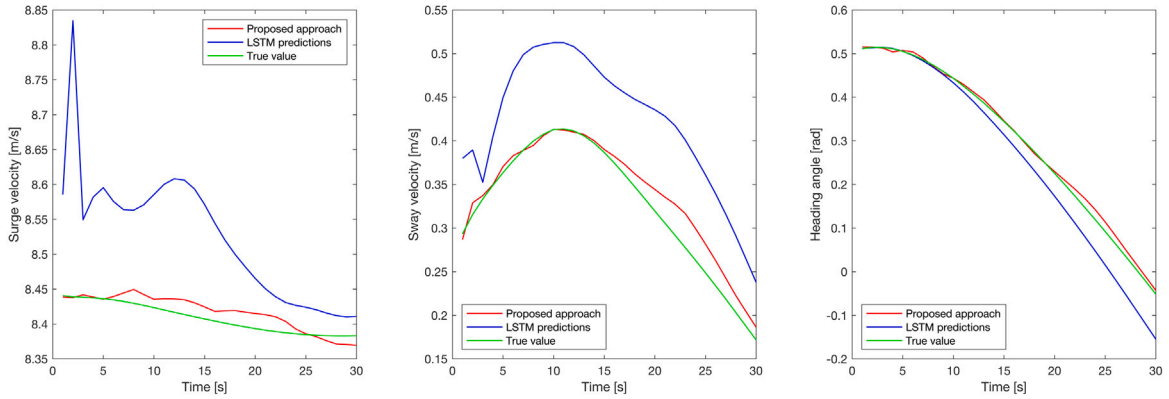

Fig. 8. The predictive velocities and heading angle of target ship in test scenario 5.

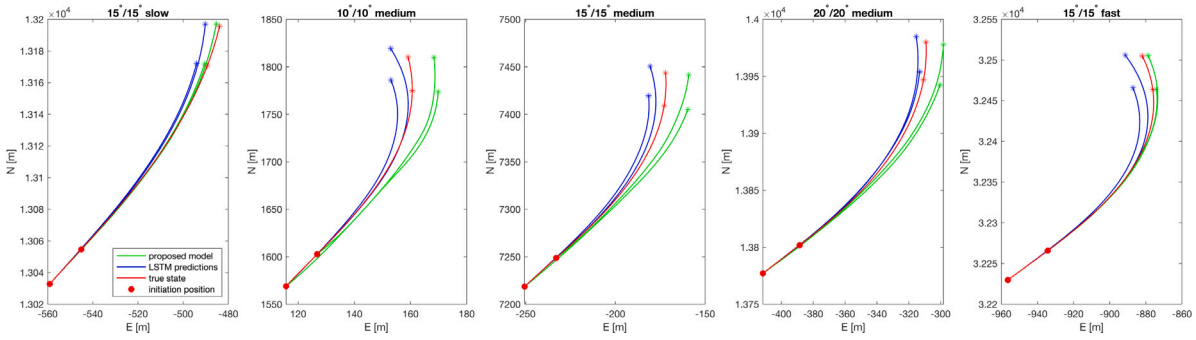

(a) Predictive trajectories when rudders turn to starboard.

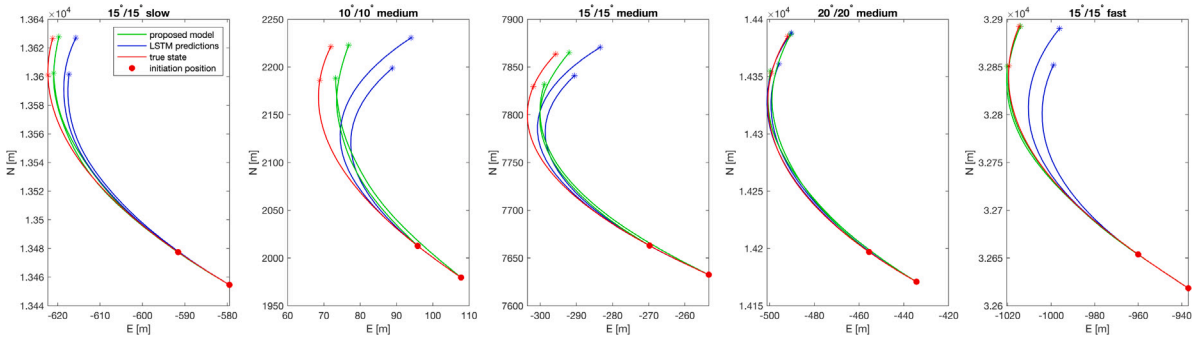

(b) Predictive trajectories when rudders turn to port side.

Fig. 9. The predictive trajectories of target ship at test scenarios.

Table 4
Predictive errors of target ship in test cases.

	Mean surge velocity error [m/s]		Mean sway velocity error [m/s]		Mean heading error [rad]		Average distance error [m]	
	Proposed	LSTM	Proposed	LSTM	Proposed	LSTM	Proposed	LSTM
15°/15° slow	0.0148	0.0569	0.0131	0.0305	0.0165	0.0593	0.4965	2.2880
10°/10° medium	0.0262	0.4033	0.0393	0.0880	0.0426	0.0982	4.4681	6.1694
15°/15° medium	0.0236	0.3009	0.0403	0.0483	0.0407	0.0694	3.5099	4.6093
20°/20° medium	0.0305	0.2542	0.0292	0.0788	0.0356	0.0360	2.4835	3.4888
15°/15° fast	0.0161	0.1516	0.0178	0.1086	0.0119	0.0947	0.6404	3.3478

5. Discussions

The experiments analyzed above evidence that by reusing and adapting the knowledge leveraged from other existing similar ships, we were able to model the target ship with limited data easily and quickly to get pleasing accuracy and generalization capability. This approach does not require a physics-based model or data-driven model built from scratch and allows us to model the target ship with limited information. When the database is not large enough to learn a complete data-driven model, such as the newly launched ship, it becomes possible to utilize the proposed strategy to develop a good enough model with informative knowledge inputs.

Yet the source ship must be carefully chosen when applying the schema because the standard features between two vessels matter greatly to the outcome models. It is accepted that knowledge transfer works before the transferred information become trustable. If the target ship is controlled in a different way from the source ship, a psudo

uniform command is required to enable the knowledge transfer. Therefore, the domain knowledge including the geometrical and propulsive characteristics has to be carefully check before the transfer action. We believe there exists a boundary of similarity that enables knowledge transfer, and the source ship to provide prior knowledge could have more choices. Thus, we would consider verifying the proposed approach on the public ship dataset to gain better generalization in future work.

One other concern about on transfer learning is that limited varied tests have been undertaken, and they do not cover the whole spectrum of maneuver conditions under which the ship may be sailing. Indeed, one general model sometimes can be less qualified to provide instructions, especially when the surrounding situations change. However we believe the proposal of multiple local models can help address this issue. Each sub-model is prepared for a specific situation, such as calm water or gentle sea states. The source model could switch among these local candidates so that the quality of transferable knowledge is ensured and predictions are rendered for as many scenarios for the target ship as possible. Integrating local source models and a finite amount of target data is expected to spare effort and hasten the modeling process compared to the classic approaches. Moreover, providing predictions with confidence awareness plays an essential role in decision support and shipping safety (Rong et al., 2019; Xue et al., 2020). To this end, in future work, we would take the prediction uncertainties into account and gain insights into the prediction confidence.

6. Conclusion

In this paper, a knowledge transfer strategy across ships is proposed aiming to reuse the information reserved in a similar ship to enhance the target ship model. Developed with physics-based and data-driven disciplines, the framework facilitates the modeling of the target ship by adapting the similar trends leveraged by the source ship with a finite amount of data. Sparing the efforts of building a physics-based or data-driven model from scratch, transferring knowledge from existing benchmark ships makes it quick and easy to achieve fine models. In this study, experiments and discussions are conducted on two real ships in practice. A characteristics vector containing the parameters impacting the ship's maneuverability is proposed to measure the similarity between ships quantitatively. The maneuverability of the two vessels is compared, and the results indicate the future trends can be transferred to the target ship. Following the proposed strategy, the discrepancies between model trends and target ship true states are calibrated by the neural network. Comparative study is conducted between the proposed approach and traditional recurrent neural network. Results show that the knowledge transfer model enables the prediction of maneuver trajectories with high accuracy and good generalizability.

As discussed, the performance of this methodology will be affected by the fidelity of the source ship. To enable the target ship model to be compatible with more complex scenarios, especially dynamic environments, more efforts are needed to exploit multiple local source models, as well as the strategy to dynamically and smoothly switch among candidate models. Thus work on developing flexible and intelligent models of ships will continue.

CRediT authorship contribution statement

Tongtong Wang: Conceptualization, Methodology, Investigation, Writing – original draft. **Robert Skulstad:** Software, Writing – review & editing. **Motoyasu Kanazawa:** Discussion, Writing – review & editing. **Guoyuan Li:** Resources, Supervision. **Houxiang Zhang:** Project administration, Supervision.

Declaration of competing interest

The authors declare that they have no known competing financial interests or personal relationships that could have appeared to influence the work reported in this paper.

Data availability

No data was used for the research described in the article.

References

Dai, S., Wang, C., Luo, F., 2012. Identification and learning control of ocean surface ship using neural networks. IEEE Trans. Ind. Inform. 8 (4), 801–810. http://dx.doi.org/10.1109/TII.2012.2205584.

Dai, S.-L., Wang, M., Wang, C., 2015. Neural learning control of marine surface vessels with guaranteed transient tracking performance. IEEE Trans. Ind. Electron. 63 (3), 1717–1727.

Gunning, D., Stefik, M., Choi, J., Miller, T., Stumpf, S., Yang, G.-Z., 2019. XAI—Explainable artificial intelligence. Science Robotics 4 (37), eaay7120.

Li, Y., Ding, Z., Zhang, C., Wang, Y., Chen, J., 2019. SAR ship detection based on resnet and transfer learning. In: IGARSS 2019-2019 IEEE International Geoscience and Remote Sensing Symposium. IEEE, pp. 1188–1191.

Li, G., Kawan, B., Wang, H., Zhang, H., 2017. Neural-network-based modelling and analysis for time series prediction of ship motion. Ship Technol. Res. 64 (1), 30–39.

NTNU, 2022. Research vessel R/V Gunnerus. URL: https://www.ntnu.edu/oceans/gunnerus.

Pan, S.J., Yang, Q., 2009. A survey on transfer learning. IEEE Trans. Knowl. Data Eng. 22 (10), 1345–1359.

Panwar, H., Gupta, P., Siddiqui, M.K., Morales-Menendez, R., Bhardwaj, P., Sharma, S., Sarker, I.H., 2020. AquaVision: Automating the detection of waste in water bodies using deep transfer learning. Case Stud. Chem. Environ. Eng. 2, 100026.

Pedregosa, F., Varoquaux, G., Gramfort, A., Michel, V., Thirion, B., Grisel, O., Blondel, M., Prettenhofer, P., Weiss, R., Dubourg, V., Vanderplas, J., Passos, A., Cournapeau, D., Brucher, M., Perrot, M., Duchesnay, E., 2011. Scikit-learn: Machine learning in python. J. Mach. Learn. Res. 12, 2825–2830.

Qiang, Z., Guibing, Z., Xin, H., Renming, Y., 2019. Adaptive neural network auto-berthing control of marine ships. Ocean Eng. 177, 40–48.

Ramirez, W.A., Leong, Z.Q., Nguyen, H., Jayasinghe, S.G., 2018. Non-parametric dynamic system identification of ships using multi-output Gaussian processes. Ocean Eng. 166, 26–36.

Rasheed, A., San, O., Kvamsdal, T., 2020. Digital twin: Values, challenges and enablers from a modeling perspective. IEEE Access 8, 21980–22012. http://dx.doi.org/10.1109/ACCESS.2020.2970143.

Rong, H., Teixeira, A., Soares, C.G., 2019. Ship trajectory uncertainty prediction based on a Gaussian process model. Ocean Eng. 182, 499–511.

Shin, J., Kwak, D.J., Lee, Y.-i., 2017. Adaptive path-following control for an unmanned surface vessel using an identified dynamic model. IEEE/ASME Trans. Mechatronics 22 (3), 1143–1153.

Skulstad, R., Li, G., Fossen, T.I., Vik, B., Zhang, H., 2019. Dead reckoning of dynamically positioned ships: Using an efficient recurrent neural network. IEEE Robot. Autom. Mag. 26 (3), 39–51. http://dx.doi.org/10.1109/MRA.2019.2918125.

Solomatine, D.P., Ostfeld, A., 2008. Data-driven modelling: some past experiences and new approaches. J. Hydroinform. 10 (1), 3–22.

Sutulo, S., Soares, C.G., 2014. An algorithm for offline identification of ship manoeuvring mathematical models from free-running tests. Ocean Eng. 79, 10–25.

Taimuri, G., Matusiak, J., Mikkola, T., Kujala, P., Hirdaris, S., 2020. A 6-DoF maneuvering model for the rapid estimation of hydrodynamic actions in deep and shallow waters. Ocean Eng. 218, 108103.

Tan, C., Sun, F., Kong, T., Zhang, W., Yang, C., Liu, C., 2018. A survey on deep transfer learning. In: International Conference on Artificial Neural Networks. Springer, pp. 270–279.

Ulstein, 2022. OLYMPIC ZEUS. URL: https://ulstein.com/references/olympic-zeus.

Wang, D., Fan, T., Han, T., Pan, J., 2020. A two-stage reinforcement learning approach for multi-UAV collision avoidance under imperfect sensing. IEEE Robot. Autom. Lett. 5 (2), 3098–3105. http://dx.doi.org/10.1109/LRA.2020.2974648.

Wang, T., Li, G., Hatledal, L.I., Skulstad, R., Æsøy, V., Zhang, H., 2021a. Incorporating approximate dynamics into data-driven calibrator: A representative model for ship maneuvering prediction. IEEE Trans. Ind. Inform. 1. http://dx.doi.org/10.1109/TII.2021.3088404.

Wang, T., Li, G., Wu, B., Æsøy, V., Zhang, H., 2021b. Parameter identification of ship manoeuvring model under disturbance using support vector machine method. Ships Offshore Struct. 16 (sup1), 13–21.

Wang, T., Skulstad, R., Kanazawa, M., Li, G., Æsøy, V., Zhang, H., 2022. Physics-informed data-driven approach for ship docking prediction. In: 2022 IEEE International Conference on Real-Time Computing and Robotics (RCAR). pp. 111–117. http://dx.doi.org/10.1109/RCAR54675.2022.9872179.

Wang, Y., Wang, C., Zhang, H., 2018. Combining a single shot multibox detector with transfer learning for ship detection using sentinel-1 SAR images. Remote Sens. Lett. 9 (8), 780–788.

Woo, J., Park, J., Yu, C., Kim, N., 2018. Dynamic model identification of unmanned surface vehicles using deep learning network. Appl. Ocean Res. 78, 123–133.

Xue, Y., Liu, Y., Ji, C., Xue, G., Huang, S., 2020. System identification of ship dynamic model based on Gaussian process regression with input noise. Ocean Eng. 216, 107862.

Yan, R., Shen, F., Sun, C., Chen, X., 2019. Knowledge transfer for rotary machine fault diagnosis. IEEE Sens. J. 20 (15), 8374–8393.

Yekeen, S.T., Balogun, A.-L., Yusof, K.B.W., 2020. A novel deep learning instance segmentation model for automated marine oil spill detection. ISPRS J. Photogramm. Remote Sens. 167, 190–200.

Yin, J., Wang, N., Perakis, A.N., 2018. A real-time sequential ship roll prediction scheme based on adaptive sliding data window. IEEE Trans. Syst. Man Cybern.: Syst. 48 (12), 2115–2125. http://dx.doi.org/10.1109/TSMC.2017.2735995.

Zhang, H., Li, G., Hatledal, L.I., Chu, Y., Ellefsen, A.L., Han, P., Major, P., Skulstad, R., Wang, T., Hildre, H.P., 2022. A digital twin of the research vessel gunnerus for lifecycle services: Outlining key technologies. IEEE Robot. Autom. Mag. 2–15. http://dx.doi.org/10.1109/MRA.2022.3217745.

Zheng, Z., Sun, L., 2016. Path following control for marine surface vessel with uncertainties and input saturation. Neurocomputing 177, 158–167.

Zheng, H., Wang, R., Yang, Y., Yin, J., Li, Y., Li, Y., Xu, M., 2019. Cross-domain fault diagnosis using knowledge transfer strategy: a review. Ieee Access 7, 129260–129290.